

Ratios of Elastic Scattering of Pions from ${}^3\text{H}$ and ${}^3\text{He}$

W. J. Briscoe, B. L. Berman, R. W. C. Carter,* K. S. Dhuga, S. K. Matthews,† and N-J. Nicholas‡
*Center for Nuclear Studies, Department of Physics,
The George Washington University, Washington DC 20052*

S. J. Greene
Los Alamos National Laboratory, Los Alamos NM 87545

B. M. K. Nefkens and J. W. Price
*Department of Physics, University of California at Los Angeles,
Los Angeles, CA 90095*

L. D. Isenhower and M. E. Sadler
*Department of Physics,
Abilene Christian University, Abilene TX 79699*

I. Šlaus and I. Supek
*Rudjer Bošković Institute, Zagreb, Croatia
(Dated: October 24, 2018)*

We have measured the elastic-scattering ratios of normalized yields for charged pions from ${}^3\text{H}$ and ${}^3\text{He}$ in the backward hemisphere. At 180 MeV, we completed the angular distribution begun with our earlier measurements, adding six data points in the angular range of 119° to 169° in the π -nucleus center of mass. We also measured an excitation function with data points at 142, 180, 220, and 256 MeV incident pion energy at the largest achievable angle for each energy – between 160° and 170° in the π -nucleus center of mass. This excitation function corresponds to the energies of our forward-hemisphere studies. The data, taken as a whole, show an apparent role reversal of the two charge-symmetric ratios r_1 and r_2 in the backward hemisphere. Also, for data $\geq 100^\circ$ we observe a strong dependence on the four-momentum transfer squared $-t$ for all of the ratios regardless of pion energy or scattering angle, and we find that the superratio R data match very well with calculations based on the forward-hemisphere data that predicts the value of the difference between the even-nucleon radii of ${}^3\text{H}$ and ${}^3\text{He}$. Comparisons are also made with recent calculations incorporating different wave functions and double scattering models.

PACS numbers: PACS numbers 25.55.Ci, 25.80.Dj, 25.10.+s, 27.10.+h, 24.80.+y

I. BACKGROUND

The first nucleus to exhibit ‘real’ nuclear properties is the three-body nucleus. There are only two stable $A = 3$ nuclei, ${}^3\text{H}$ and ${}^3\text{He}$; neither member of this isospin doublet has any known excited state. The ground state of ${}^3\text{H}$ has one proton and two spin-paired neutrons, while that of ${}^3\text{He}$ has one neutron and two spin-paired protons. We refer to the neutrons in ${}^3\text{H}$ and the protons in ${}^3\text{He}$ as the ‘even’ nucleons, and to their *rms* radii as

the even radii for ${}^3\text{H}$ and ${}^3\text{He}$, respectively. Similarly, the proton in ${}^3\text{H}$ and the neutron in ${}^3\text{He}$ are called ‘odd’ nucleons and their *rms* radii shall be referred to as odd radii [1]. Charge symmetry requires that, in the absence of Coulomb effects and mass differences, these nuclei be identical. This is because ${}^3\text{H}$ and ${}^3\text{He}$ are mirror nuclei and are related by a 180° rotation in isospin space, or to put it more simply, one nucleus changes into the other by interchange of neutrons and protons.

There are four interactions available between the two charged pions and ${}^3\text{H}$ and ${}^3\text{He}$ target nuclei. These are grouped conveniently in ‘isospin’ pairs $\pi^+{}^3\text{H}$ and $\pi^-{}^3\text{He}$, $\pi^-{}^3\text{H}$ and $\pi^+{}^3\text{He}$ which in turn are related to each other by the interchange of protons with neutrons and π^+ with π^- . *In the absence of the Coulomb force*, if the strong interaction is charge symmetric, scattering cross sections for the members of each of these pairs should be equal.

If we make the assumption that an incident pion interacts with a single target nucleon, then we can look at

*Present address: 1627 Camden Ave. # 307, Los Angeles, CA 90025

†Present address: Oregon Hearing Research Center, Oregon Health Science University Portland, OR 97201-3098

‡Present address: Advanced Nuclear Technology Group (NIS-6), MS J562, Nonproliferation and International Security Division, LANL, Los Alamos, NM 87545

these interactions in terms of π -nucleon scattering amplitudes. At 180 MeV (near the peak of the Δ_{33} resonance) the π^+p (π^-n) scattering amplitude is about three times as large as the π^+n (π^-p). Consequently, the elastic cross sections for π^+p and π^-n are nine times as large as those for π^+n and π^-p . The π -N scattering amplitudes can be broken down into *spin-flip* and *non-spin-flip* components. For a fixed target nucleon and pions of 180 MeV, the *spin-flip* amplitude has a sine dependence on the scattering angle; the *non-spin-flip* amplitude has a cosine dependence. Since no excited states are available, single *spin-flip* scattering from one of the even nucleons would leave both nucleons with the same spin and is thus forbidden by the Pauli principle. (See Ref. [2] for further discussion on this point.)

However, at the large scattering angles $\geq 100^\circ$ for which our most recent data were obtained, kinematic considerations require that one consider double- or multiple-scattering effects. This would open the door to double spin-flip scattering in the even nucleons which would not violate the Pauli principle. The description of the whole picture is discussed in the accompanying article of Kudryavtsev *et al.* [3]. Pion-nuclear amplitudes, discussed in [3], are a superposition of a single- and double-scattering of pions from the nucleons in the nucleus with Fermi motion taken into account. Principal sources of the violation of charge symmetry in [3] are (i) the Coulomb interaction between the charged pions and the nuclei (the external Coulomb effect), (ii) n-p doublet and the mass splitting of the different charged states of the Δ_{33} -isobar, and (iii) the difference between the wave functions of 3H and 3He due to the additional Coulomb repulsion between the two protons in the 3He nucleus (the internal Coulomb effect.)

Several ratios of scattering cross sections have been defined in conjunction with our earlier measurements [2, 4, 5, 6] in order to highlight certain features of the π - 3A interaction.

The first two are the *charge-symmetric* ratios

$$r_1 = \frac{d\sigma(\pi^+{}^3H)}{d\sigma(\pi^-{}^3He)} \quad (1)$$

and

$$r_2 = \frac{d\sigma(\pi^-{}^3H)}{d\sigma(\pi^+{}^3He)}. \quad (2)$$

The numerator and denominator of each pair are related by an exchange of protons with neutrons and π^+ with π^- . Therefore, the strong interactions in the denominator and numerator are equal, and these ratios should be identically one at all energies and four-momentum transfers squared. However, since the form factor of 3He is decreased owing to the Coulomb repulsion between its protons, the cross section in the denominator is reduced and we expect that the ratios r_1 and r_2 will be somewhat greater than one [7, 8]. In r_1 , scattering from the odd nucleon dominates in the delta energy region, and so the

scattering is a mixture of spin-flip and non-spin-flip. In r_2 , scattering from the even nucleon dominates, and so spin-flip scattering is suppressed.

The next ratio is R , the ‘‘superratio.’’ It is defined as the product of r_1 and r_2 ,

$$R = r_1 \cdot r_2. \quad (3)$$

Since r_1 and r_2 are charge symmetric, so is R .

Finally, we define

$$\rho^+ = \frac{d\sigma(\pi^+{}^3H)}{d\sigma(\pi^+{}^3He)} \quad (4)$$

and

$$\rho^- = \frac{d\sigma(\pi^-{}^3H)}{d\sigma(\pi^-{}^3He)}. \quad (5)$$

These ratios are not charge symmetric, but, as shall be seen below, several experimental uncertainties cancel when calculating ρ^+ and ρ^- , and they can be used to derive the charge-symmetric R , where

$$R = \rho^+ \cdot \rho^-. \quad (6)$$

In Section II, we briefly discuss the analysis of our data at energies spanning the Δ_{33} resonance. The resulting charge-symmetric ratios r_1 and r_2 , non charge-symmetric ratios ρ^+ and ρ^- , and Superratio R are presented in Section III. In Section IV, we discuss the situation for angles greater than 100° . Finally, we summarize our findings in Section V.

II. EXPERIMENT

The experimental details have been given by Matthews *et al.* [9]. Here, we briefly discuss the analysis of the data and the relevant experimental parameters for the determination of the scattering ratios.

The ratios r_1 and r_2 are extracted as

$$r_1 = \frac{Y(\pi^+{}^3H)}{Y(\pi^+{}^2H)} \cdot \frac{Y(\pi^-{}^2H)}{Y(\pi^-{}^3He)} \cdot \frac{d\sigma(\pi^+{}^2H)}{d\sigma(\pi^-{}^2H)} \cdot \frac{N_{3He}}{N_{3H}} \quad (7)$$

and

$$r_2 = \frac{Y(\pi^-{}^3H)}{Y(\pi^-{}^2H)} \cdot \frac{Y(\pi^+{}^2H)}{Y(\pi^+{}^3He)} \cdot \frac{d\sigma(\pi^-{}^2H)}{d\sigma(\pi^+{}^2H)} \cdot \frac{N_{3He}}{N_{3H}}, \quad (8)$$

where $Y(\pi^\pm {}^nA)$ refers to the scattering yield, and N_{3H} and N_{3He} are the number of scattering centers per unit volume in the 3H and 3He samples, respectively. These latter were measured very accurately – see Ref. [9] for details. Elastic scattering yields from 2H are used to scale the other yields to the known $\pi^\pm {}^2H$ cross sections. Writing the ratio $d\sigma(\pi^+{}^2H)/d\sigma(\pi^-{}^2H)$ as D , and defining Y_N as the yield per target nucleon $Y(\pi^\pm {}^nA)/N_A$, we have

$$r_1 = \frac{Y_N(\pi^+{}^3H) \cdot Y(\pi^-{}^2H) \cdot D}{Y_N(\pi^-{}^3He) \cdot Y(\pi^+{}^2H)} \quad (9)$$

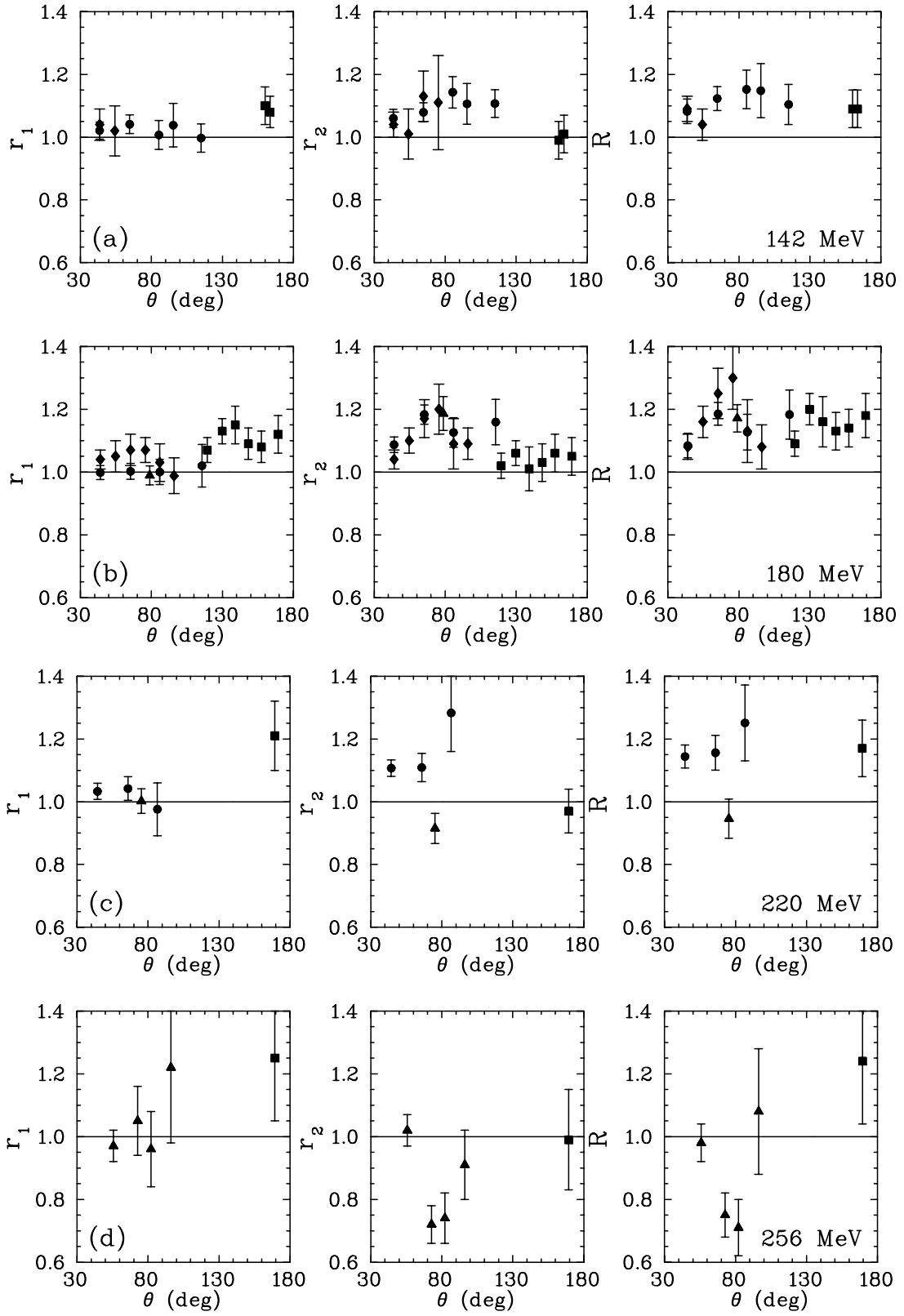


FIG. 1: The ratios r_1 , r_2 , and the Superratio R for $\pi^\pm {}^3\text{H}/{}^3\text{He}$ elastic scattering plotted versus the center-of-mass angle in the $\pi - {}^3\text{A}$ system for various incident pion kinetic energies: (a) $T_\pi = 142$ MeV, (b) 180 MeV, (c) 220 MeV, and (d) 256 MeV. Experimental data are from [4] (diamonds), [2] (circles), [6] (triangles), and this experiment (squares).

TABLE I: Measured values of the ratios from this experiment. The quoted uncertainties are statistical only.

| $T_\pi(\text{MeV})$ | $\theta(\text{deg})$ | $-t(\text{fm}^{-2})$ | ρ^+ | ρ^- | r_1 | r_2 | R |
|---------------------|----------------------|----------------------|--------------|--------------|------------|------------|------------|
| 142 | 160.0 | 5.0 | 0.811(0.024) | 1.347(0.065) | 1.10(0.06) | 0.99(0.06) | 1.09(0.06) |
| 142 | 163.6 | 5.0 | 0.757(0.027) | 1.401(0.086) | 1.08(0.05) | 1.01(0.06) | 1.09(0.06) |
| 180 | 119.4 | 5.2 | 0.85 (0.02) | 1.28 (0.04) | 1.07(0.04) | 1.02(0.04) | 1.09(0.04) |
| 180 | 129.8 | 5.7 | 0.87 (0.02) | 1.38 (0.04) | 1.13(0.04) | 1.06(0.04) | 1.20(0.05) |
| 180 | 139.1 | 6.1 | 0.75 (0.03) | 1.56 (0.08) | 1.15(0.06) | 1.01(0.07) | 1.16(0.08) |
| 180 | 148.3 | 6.4 | 0.55 (0.02) | 2.05 (0.09) | 1.09(0.05) | 1.03(0.06) | 1.13(0.06) |
| 180 | 157.4 | 6.7 | 0.44 (0.01) | 2.62 (0.11) | 1.08(0.05) | 1.06(0.06) | 1.14(0.06) |
| 180 | 169.2 | 6.9 | 0.38 (0.01) | 3.06 (0.15) | 1.12(0.06) | 1.05(0.06) | 1.18(0.06) |
| 220 | 169.3 | 8.9 | 0.408(0.035) | 2.86 (0.18) | 1.21(0.11) | 0.97(0.07) | 1.17(0.09) |
| 256 | 169.4 | 10.9 | 0.478(0.035) | 2.59 (0.37) | 1.25(0.20) | 0.99(0.16) | 1.24(0.20) |

and similarly

$$r_2 = \frac{Y_N(\pi^{-3}H) \cdot Y(\pi^{+2}H)}{Y_N(\pi^{+3}He) \cdot Y(\pi^{-2}H) \cdot D}. \quad (10)$$

Then

$$R = \frac{Y_N(\pi^{+3}H) \cdot Y_N(\pi^{-3}H)}{Y_N(\pi^{-3}He) \cdot Y_N(\pi^{+3}He)}. \quad (11)$$

All normalization quantities not related to N_{3H} and N_{3He} cancel in R . In the definitions of r_1 and r_2 , it is the *ratio* of the $\pi^{\pm 2}H$ yields and cross sections that appears.

Finally, we consider the ratios ρ^+ and ρ^- . Since the same charge of pion appears in both the numerator and denominator of each of these ratios, the non-target-related normalization quantities cancel here as well. Then we have

$$\rho^+ = \frac{Y_N(\pi^{+3}H)}{Y_N(\pi^{+3}He)} \quad (12)$$

and

$$\rho^- = \frac{Y_N(\pi^{-3}H)}{Y_N(\pi^{-3}He)}, \quad (13)$$

so that

$$R = r_1 \cdot r_2 = \rho^+ \cdot \rho^-. \quad (14)$$

III. RATIOS

Values for all of the ratios measured in this experiment are given in Table I. Figure 1 shows the angular distributions for the simple charge-symmetric ratios r_1 , r_2 , and the superratio R at 142, 180, 220, and 256 MeV. We see that r_1 is flat and structureless in the forward hemisphere but rises in the backward hemisphere where it remains high to 180°. The ratio r_2 shows structure at about 80° in the forward hemisphere, approaches 1.0 in

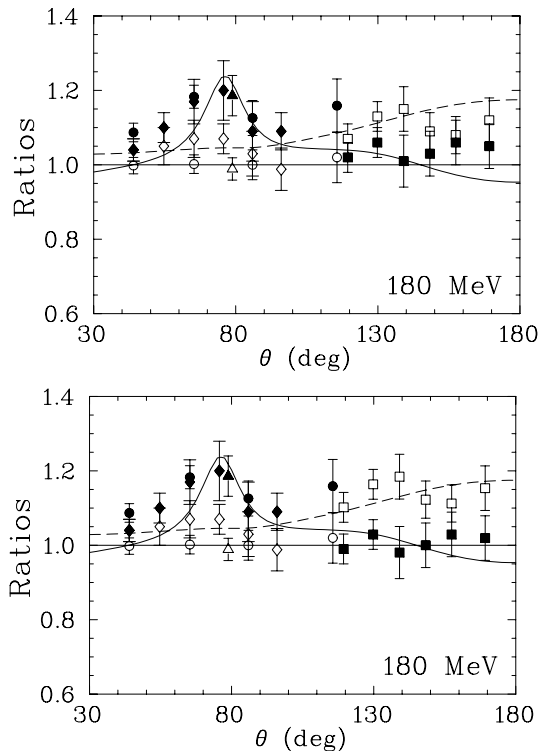


FIG. 2: The simple ratios r_1 (open symbols) and r_2 (filled symbols) are compared to the calculations of Ref. [3] for r_1 (dashed line) and r_2 (solid line). The qualitative behavior of the simple ratios, including the crossover, were predicted by an optical-model calculation by Gibbs and Gibson [10] before the back-angle data were taken. In the top figure, we used the assumption that the yield for π^+d/π^-d is equal to 1.00 as is indicated by the SAID fit to the $\pi-d$ data [11]. In the bottom figure, we used the results of Smith *et al.* [12] which give a value of 1.03 for this ratio at back angles. A slight improvement of the χ^2 is obtained using the value 1.03. The simple ratios cross in the region where double and multiple scattering begin to become more important in the scattering process.

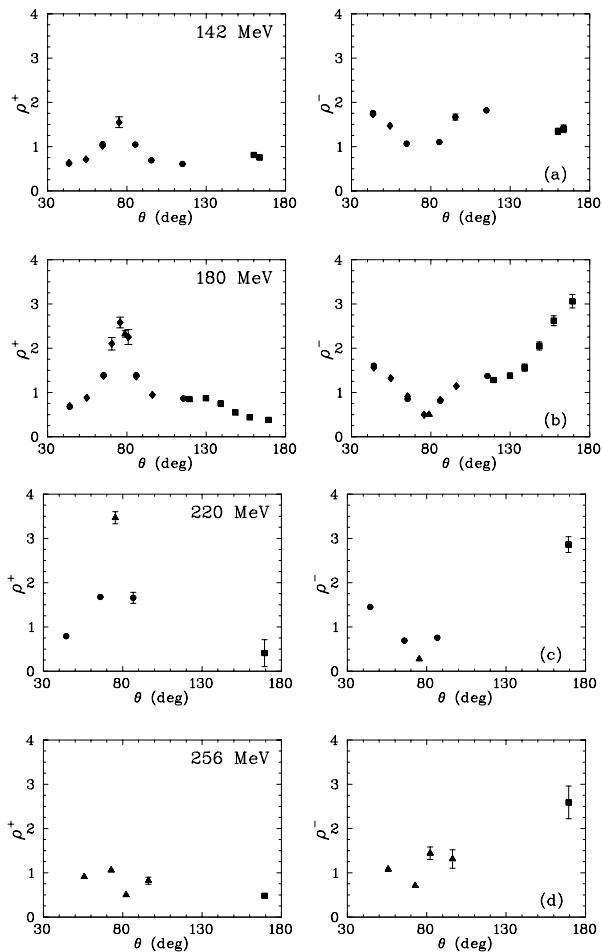


FIG. 3: The ratios ρ^+ and ρ^- for (a) $T_\pi = 142$ MeV, (b) 180 MeV, (c) 220 MeV, and (d) 256 MeV. The notation for the experimental data is the same as for Fig. 1.

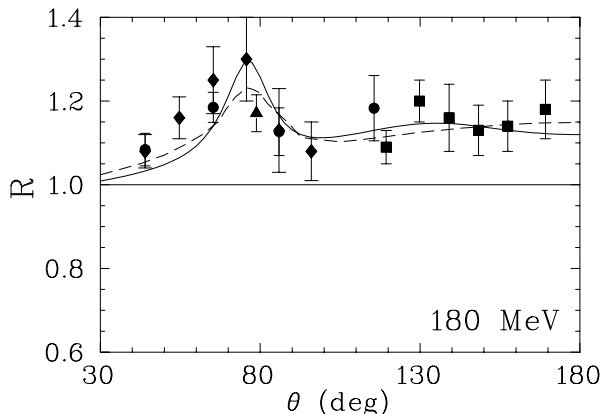


FIG. 4: The Superratio R at $T_\pi = 180$ MeV is compared to calculations by Kudryavtsev *et al.* [3] (solid curve) and Gibbs and Gibson [10] (dashed curve). The notation for the experimental data is the same as in Fig. 1.

the backward hemisphere and stays there to 180° . Most of the structure in R is therefore due to r_2 .

We note that, aside from the region near 80° in the $\pi - {}^3\text{A}$ center-of-mass kinematics, which corresponds to 90° in the $\pi - N$ center of mass where the non-spin-flip scattering amplitudes have zeros, the charge-symmetric scattering ratios do not have any sharp features. Indeed, in the backward hemisphere they are fairly flat and quite smooth. This is not surprising, since the π -nucleon amplitudes are smooth and have no zeros in this region. The form factors for ${}^3\text{H}$ and ${}^3\text{He}$, as measured with electron scattering, are smooth as well. Finally, the interactions in the numerator and denominator for each ratio are approximately the same: primarily odd-nucleon in r_1 , and primarily even-nucleon in r_2 . R is the smooth product of two smooth functions.

Of more interest is the general trend of the ratios as we progress from the forward to the backward hemispheres, see Fig. 2. The crossover of the two ratios, and the fact that r_1 is significantly different from unity but r_2 is consistent with unity is difficult to explain quantitatively. It is interesting to note that the qualitative behavior of the simple ratios, including the crossover, were predicted by an optical-model calculation by Gibbs and Gibson [10] before the back-angle data were taken.

One might speculate that as one passes to the backward hemisphere, with the diminishing importance of the single-scattering process, the double-scattering process provides a mechanism for spin-flip amplitudes to contribute in paired-nucleon scattering without violating the Pauli exclusion principle. In the top plot of Fig. 2, we assume that $d\sigma(\pi^+{}^2\text{H}) = d\sigma(\pi^-{}^2\text{H})$. In the bottom plot, we assume the 1.5% asymmetry suggested by Smith *et al.* [12] for $\theta \geq 90^\circ$, which means correcting the value of D by 3%. The effect is to *increase* the difference between r_1 and r_2 in the backward hemisphere.

Figure 3 shows results for ρ^+ and ρ^- . These ratios have very small error bars, owing to the cancellation of normalization quantities mentioned above. The steep rise of ρ^- and the fall below one of ρ^+ are indications that there is a steep rise in the 180-MeV even-nucleon-dominated cross sections at large angles [9]. However, the error bars for these ratios are much smaller than those for the cross sections. These ratios are the most sensitive test of the large-angle scattering calculations; in particular, these test the form factors used in the calculation.

Figure 4 shows R at 180 MeV. The shape is derived from the two simple ratios, the bump at 80° corresponding to the bump in r_2 and the steady rise in the backward hemisphere to the rise in r_1 . Figure 4 also shows the calculations by Kudryavtsev *et al.* [3] and by Gibbs and Gibson [10]. In the latter the shape of the Superratio was used to extract differences in the odd and even nucleon radii more precisely than is possible from existing electron scattering data. Gibbs' and Gibson's optical-model calculation shows a strong dependence on two parameters, the difference between the *rms* neutron radius in tritium and the *rms* proton radius in ${}^3\text{He}$ (that is, the

difference in the even-nucleon radii), and the difference between the *rms* proton radius in 3H and the *rms* neutron radius in 3He . In the approach of Ref. [3], a successful description of R at $T_\pi = 180$ MeV is based not only on the difference in the wave functions of 3H and 3He , but also on the Δ_{33} mass splitting as well as on the inclusion of the double-scattering interaction of the pion with nucleons of the target nuclei. Both models account for the role reversal of the r_1 and r_2 at back angles for the $T_\pi = 180$ MeV. However, Kudryavtsev *et al.* fitted r_1 and r_2 to determine R , while Gibbs and Gibson fitted their calculations to R and inferred r_1 and r_2 prior to the time that the data were obtained.

Although the leading terms included in the calculation of Kudryavtsev *et al.* reproduce the main features of the back-angle ratios at energies of 180 MeV and above, yet another factor which might contribute to this remarkable role reversal of r_1 and r_2 at back angles is a two-step process consisting of the formation of a virtual delta by the interaction of the incident pion with a nucleon, followed by the scattering of this delta on the remaining correlated nucleon pair. This process is clearly overshadowed by single scattering at angles near the non-spin-flip dip, but, like any two-step process, could become important as the momentum transfer increases.

For r_1 , the dominant channels for delta formation would be $\pi^+ + p \rightarrow \Delta^{++}$ in the numerator and $\pi^- + n \rightarrow \Delta^-$ in the denominator, whereas the reverse would be the case for r_2 . [For r_1 the correlated pairs would be (nn) in the numerator and (pp) in the denominator, and for r_2 they would be (np) pairs in both numerator and denominator.] Since the width of the Δ^{++} is somewhat smaller than that of the Δ^- (about 5 MeV out of a total width of about 120 MeV Ref. [13]), the lifetime of the former would be longer than that of the latter, and likewise its interaction cross section with the (NN) pair would be larger. Thus, at back angles, where this effect might become increasingly important, it would have the effect of increasing r_1 and decreasing r_2 , which corresponds to their observed behavior.

IV. DEPENDENCE ON MOMENTUM TRANSFER

Figure 5 shows r_1 , r_2 , and R at the large scattering angles ($\geq 100^\circ$) for all pion energies plotted versus the four-momentum transfer squared. In Fig. 5a, r_1 increases steadily, while in Fig 5b, r_2 decreases slightly with $-t$. R displays a very slight increase with the four-momentum transfer squared, as shown in Fig. 5c. From Fig. 5 one can conclude that, since r_1 , r_2 , and R , coming from different energy sets, fall on top of each other and follow the same general trend, these ratios are primarily functions of $-t$.

The behavior of ρ^+ and ρ^- at the largest scattering angles versus T_π can be analyzed with the help of Table 1. As is seen in the table, ρ^+ decreases sharply from 142 to 180 MeV, then rises slightly through 220

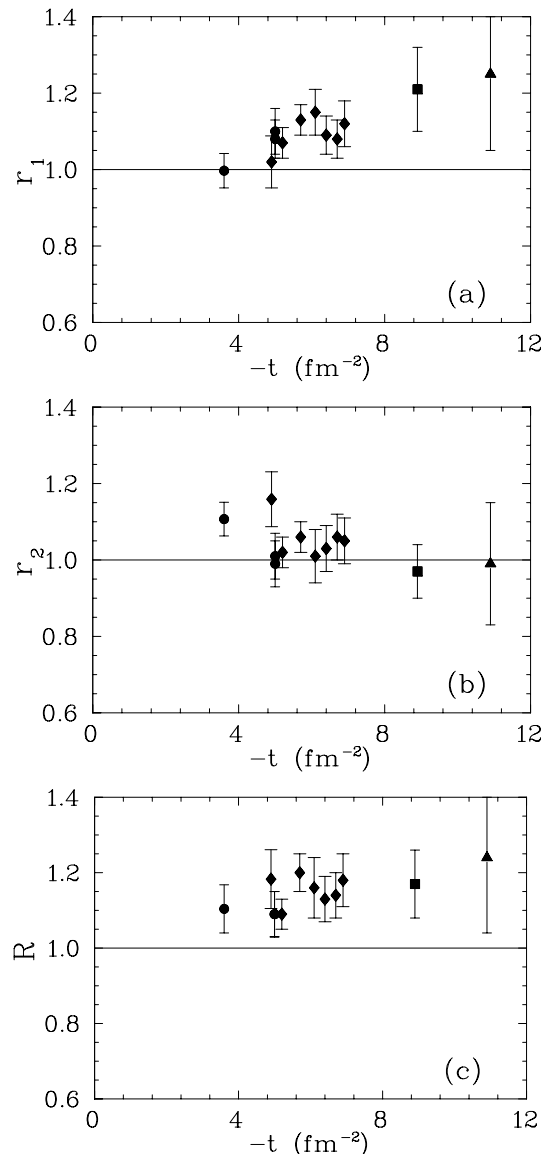


FIG. 5: The excitation function for the ratios (a) r_1 , (b) r_2 , and (c) R at back angles ($\geq 100^\circ$) are shown versus the four-momentum transfer squared $-t$. Experimental data are from [2, 4, 6] and present experiment [142 MeV data are shown by circles, 180 MeV data by diamonds, 220 MeV data by squares, and 256 MeV data by triangles].

and 256 MeV. ρ^- shows the opposite behavior, with a maximum at 180 MeV. The excitation functions for ρ^+ and $1/\rho^-$ for backward angles versus $-t$ are shown in Fig. 6. As is the case for r_1 , r_2 , and R , the agreement of the overlaid data at different energies is also quite good.

We note that in the forward hemisphere, a model that assumes single $\pi - N$ scattering explains the behavior of elastic $\pi - {}^3A$ scattering quite nicely, and the reaction is completely defined by $\pi - {}^3A$ kinematics. However, for angles greater than 100° , kinematic considerations force us to consider two-step processes, especially double scattering to explain $\pi - {}^3A$ elastic scattering and all of the

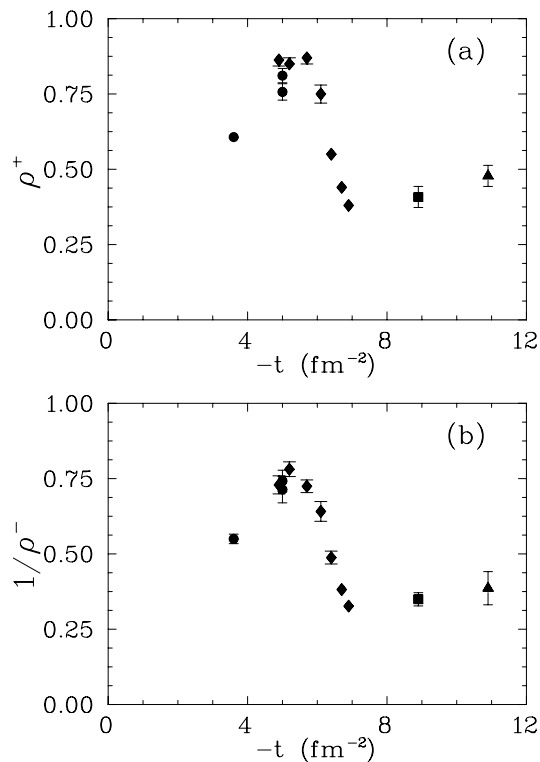


FIG. 6: The excitation function for the ratios (a) ρ^+ and (b) $1/\rho^-$ at back angles ($\geq 100^\circ$) are shown versus the four-momentum transfer squared $-t$. The notation for the experimental data is the same as in Fig. 5.

ratios are seen to be smooth functions of the momentum transfer.

V. CONCLUSIONS

Several new measurements of the ratios r_1 , r_2 , and R at energies $T_\pi = 142, 180, 220,$ and 256 MeV at

backward scattering angles are presented. These data complete our previous data sets at smaller angles and the same energies [2, 4, 5, 6]. Where data sets overlap they are consistent with each other. At $T_\pi = 180$ MeV, the charge-symmetric ratios r_1 , r_2 , and R are smooth functions of the scattering angle in the backward hemisphere. The ratios r_1 and r_2 cross each other at around 120° ; r_1 becomes significantly different from 1.00 at backward angles while r_2 , which had been greater than 1.00 at forward angles, approaches unity. Deviation of the ratios r_1 , r_2 , and R from unity gives evidence for charge-symmetry-violation effects in these reactions. All three ratios, at energies of 180, 220, and 256 MeV, are well described by the theoretical approach of Ref. [3]. Additionally, the ratios at 180 MeV match well with the results of a previous calculation [10] that determines the value of the difference between the even and odd radii of ${}^3\text{He}$ and ${}^3\text{H}$. It also has been shown that all three ratios r_1 , r_2 , and R (as well as ρ^+ and ρ^-) at large scattering angles ($\geq 100^\circ$) and for all of the incident pion energies studied can be described as a function of only the four-momentum transfer squared $-t$ in the region where two-step processes such as double scattering dominate the $\pi - {}^3\text{A}$ elastic scattering.

VI. ACKNOWLEDGMENTS

The authors acknowledge the support of the US National Science Foundation, the US Department of Energy, and the GW Research Enhancement Fund. We wish to thank R. Boudrie, C. Morris, and S. Dragic for their assistance during the running of the experiment and A. E. Kudryavtsev and I. I. Strakovsky for a careful reading of the manuscript and for fruitful discussions.

-
- [1] L. I. Schiff, Phys. Rev. **113**, B802 (1964).
 - [2] C. Pillai, D. B. Barlow, B. L. Berman, W. J. Briscoe, A. Mokhtari, B. M. K. Nefkens, and M. E. Sadler, Phys. Rev. C **43**, 1838 (1991).
 - [3] A. E. Kudryavtsev, V. E. Tarasov, B. L. Berman, W. J. Briscoe, K. S. Dhuga, and I. I. Strakovsky, submitted to Phys. Rev. C.; Eprint nucl-th/0109074.
 - [4] B. M. K. Nefkens, W. J. Briscoe, A. D. Eichen, D. H. Fitzgerald, A. Mokhtari, J. A. Wightman, and M. E. Sadler, Phys. Rev. C **41**, 2770 (1990).
 - [5] W. J. Briscoe, B. L. Berman, R. W. Caress, K. S. Dhuga, S. Dragic, D. Knowles, D. Macek, S. K. Matthews, N. J. Nicholas, M. F. Taragin, D. B. Barlow, B. M. K. Nefkens, C. Pillai, J. Price, L. D. Isenhower, M. E. Sadler, S. J. Greene, I. Slaus, and I. Supek, Nucl. Phys. **A553**, 585 (1993).
 - [6] K. S. Dhuga, B. L. Berman, W. J. Briscoe, R. W. Caress, S. K. Matthews, D. B. Barlow, B. M. K. Nefkens, C. Pillai, J. W. Price, S. J. Greene, I. Slaus, and I. Supek, Phys. Rev. C **54**, 2823 (1996).
 - [7] K. Y. Kim, Y. E. Kim, and R. H. Landau, Phys. Rev. C **36**, 2155 (1987); Y. E. Kim, M. Krell, and L. Tiator, Phys. Lett. **B172**, 287 (1986); Y. E. Kim, Phys. Rev. Lett. **53**, 1508 (1984).
 - [8] W. J. Briscoe and B. H. Silverman, Phys. Rev. C **39**, 282 (1987).
 - [9] S. K. Matthews, W. J. Briscoe, C. Bennhold, B. L. Berman, R. W. Caress, K. S. Dhuga, S. N. Dragic, S. S. Kamalov, N. J. Nicholas, M. F. Taragin, L. Tiator, D. B. Barlow, B. M. K. Nefkens, C. Pillai, J. W. Price, L. D. Isenhower, M. E. Sadler, I. Slaus, and I. Supek, Phys. Rev. C **51**, 2534, 1995; and S. K. Matthews, Ph.D.

- Thesis, The George Washington University, 1992 (unpublished).
- [10] W. R. Gibbs and B. F. Gibson, *Phys. Rev. C* **43**, 1012 (1991); and private communication.
- [11] R. A. Arndt, I. I. Strakovsky, and R. L. Workman, *Phys. Rev. C* **50**, 1796 (1994).
- [12] G. R. Smith, D. R. Gill, D. Ottwell, G. D. Wait, P. Walden, R. R. Johnson, R. Olszewski, R. Rui, M. E. Sevier, R. P. Trelle, J. Brack, J. J. Kraushaar, R. A. Ristinen, H. Chase, E. L. Mathie, V. Pafis, R. B. Shubank, N. R. Stevenson, A. Rinat, and Y. Alexander, *Phys. Rev. C* **38**, 240 (1988).
- [13] D. E. Groom *et al.*, *Review of Particle Physics*, *Eur. Phys. J. C* **15**, 1 (2000), and 2001 off-year partial update for 2002 edition available on the PDG site <http://pdg.lbl.gov>.